Journal of Zhejiang University SCIENCE A
ISSN 1673-565X (Print); ISSN 1862-1775 (Online)
www.zju.edu.cn/jzus; www.springerlink.com
E-mail: jzus@zju.edu.cn

Eccentricity and thermoviscous effects on ultrasonic scattering from a liquid-coated fluid cylinder

Seyyed M. HASHEMINEJAD†, M. A. ALIBAKHSHI

(*Acoustics Research Lab., Department of Mechanical Engineering, Iran University of Science and Technology, Narmak, Tehran 16844, Iran*)

†E-mail: hashemi@iust.ac.ir

Received Feb. 10, 2007; revision accepted July 15, 2007; published online Nov. 10, 2007

Abstract: Calculation of the scattered field of the eccentric scatterers is an old problem with numerous applications. This study considers the interaction of a plane compressional sound wave with a liquid-encapsulated thermoviscous fluid cylinder submerged in an unbounded viscous thermally conducting medium. The translational addition theorem for cylindrical wave functions, the appropriate wave field expansions and the pertinent boundary conditions are employed to develop a closed-form solution in the form of infinite series. The analytical results are illustrated with a numerical example in which the compound cylinder is insonified by a plane sound wave at selected angles of incidence in a wide range of dimensionless frequencies. The backscattered far-field acoustic pressure amplitude and the spatial distribution of the total acoustic pressure in the vicinity of the cylinder are evaluated and discussed for representative values of the parameters characterizing the system. The effects of incident wave frequency, angle of incidence, fluid thermoviscosity, core eccentricity and size are thoroughly examined. Limiting case involving an ideal compressible liquid-coated cylinder is considered and fair agreement with a well-known solution is established.

Key words: Thremoviscous effects, Eccentric fluid cylinder, Acoustic scattering
doi:10.1631/jzus.A072053 **Document code:** A **CLC number:** TB5

INTRODUCTION

Historically, sound wave scattering by cylindrical objects has been investigated quite extensively since works of Rayleigh (1945) and Lamb (1945). For example, the scattering of acoustic waves has been broadly studied for a rigid, fixed, solid circular cylinder (Morse and Ingard, 1968), for elastic solid circular cylinder (Faran, 1951; Varadan *et al*., 1991), and for elastic cylindrical shells (Hasegawa *et al*., 1993). On the other hand, analytical or numerical solutions to sound wave interaction problems involving cylindrical fluid obstacles seem to be relatively sparse. Alemar *et al*.(1986a; 1986b) investigated the scattering of acoustic waves from an infinite cylindrical fluid obstacle immersed in a fluid loading medium of greater/smaller density. Chandra and Thompson (1992) employed the method of Padé approximants to determine the scattered pressure from a fluid cylinder having a strong compressibility contrast. Boag *et al*.(1988) used a multifilament source model to present a solution for the problem of 2D acoustic scattering from homogeneous fluid cylinders. Rousselot (1994) also studied the acoustic field scattered by a fluid cylinder. More recently, Wei *et al*.(2004) analyzed and discussed the acoustic radiation force on a 2D infinitely long fluid cylinder placed in a plane standing wave field. Also, Scotti and Wirgin (2004) studied the inverse medium problem (i.e., the retrieval of the material constants) for a generally-lossy fluid-like circular cylindrical object in a lossless fluid-like host probed by plane-wave acoustic radiation.

Analytical solutions of interior or exterior boundary value problems in various fields such as potential theory, acoustics and electromagnetism, are strictly dependent on the shape of boundaries. In particular, when multiple interfaces are present in a sound field, there is an acoustical interaction between them due to cross scattering. Several researchers have

studied the acoustic interaction problems involving multiple cylindrical interfaces. Shaw and Tai (1974) used Helmholtz integral equation formulation to study acoustic radiation due to a time harmonic pressure applied at the inner boundary of an acoustic fluid body composed of two parallel, nonconcentric circular cylinders. Kanevskii and Surikov (1976) theoretically and experimentally investigated the field in the focal plane of cylindrical two-layer acoustic lenses formed by two concentric layers with different refractive indices. Reese and Thompson (1986) used the translational addition theorem for cylindrical wave functions to investigate the effect of a variable thickness, cylindrical, fluid layer on the directional response patterns of a particular acoustic source distribution. Sinai and Waag (1988) employed a series solution for scattering from two concentric fluid cylinders to compute the scattered pressure for a range of frequencies and material parameters. Schuster (1990) presented a fast exact numerical algorithm that computes the line source acoustic response of concentric cylinders filled with acoustic material of contrasting impedances. Janele *et al*.(1991) considered the finite amplitude wave propagation which is created when a compound cylinder consisting of two concentric, isotropic compressible cylinders is subjected to a sudden spatially uniform application of pressure at the inner cylinder's surface. Morse *et al*.(1995) showed that scattering by a nonconcentric circular cylinder exhibits scattering processes not present in the simple case of uniform thickness. Roumeliotis and Kakogiannos (1995) used the translational addition theorems for cylindrical wave functions to study scattering of an acoustic plane wave from an infinite circular impenetrable or penetrable cylinder of an acoustically small radius, embedded eccentrically into a penetrable cylinder. Danila *et al*.(1995; 1998) used the generalized Debye series expansion (GDSE) method for calculation of the scattered field due to a plane wave incident on concentric or eccentric fluid/solid cylindrical interfaces. Hasheminejad and Azarpeyvand (2003) presented an exact analysis of acoustic radiation from a vibrating cylindrical source eccentrically suspended within a fluid cylinder. Cai (2004) reviewed and presented a novel multiple-scattering approach for analyzing scattering by single multilayered 2D scatterers having internal delineative interfaces. He used a simple two-layered concentric circular cylindrical scatterer subjected to SH incident waves in 2D space (with a known exact analytical solution) to illustrate his detailed solution procedure.

The mechanical behavior of a freely floating or captured liquid system finds application not only in mechanical sciences and metallurgy but also in chemical engineering and nuclear technology as well as in geological and astrophysical engineering (e.g., in applications where materials must be manipulated, heated or cooled without contact between the material and container walls such as in containerless solidification (Gao and Wei, 1999), crystal growth (Chung and Trinh, 1998), magnetically levitated pipeless fluid transporting system (Mai *et al*., 2002), material property measurement and material processing (Rhim *et al*., 1999), medical industry (Lorber and Giege, 1996), microstructure control of materials (Nagashio *et al*., 1999) and biological applications (Lane *et al*., 1999)). In particular, stability and dynamics of the so-called liquid bridge or column (i.e. a cylindrical mass of liquid surrounded by an immiscible host liquid with similar density to compensate partially for the effect of the hydrostatic pressure along the interface) have been extensively analyzed both theoretically and experimentally over the last decades (Sanz, 1985; Perales and Meseguer, 1992; Zayas *et al*., 2000; Montanero *et al*., 2002; Johnson, 2002; Montanero, 2003). Likewise, mechanical behaviours of liquid-encapsulated or multilayer liquid columns (i.e., a liquid column composed of two concentric immiscible viscous liquids: an inner column of liquid, forming an axisymmetric interface with an outer annular column of liquid, surrounded by the external still fluid) have recently become of great practical interest in space (containerless) material processing applications (Walker *et al*., 2002). By liquid encapsulation in microgravity conditions, the thermocapillary (Marangoni) convection in the material's melt phase can be suppressed and, in consequence of stringent control of melt stochiometry, striation-free high-purity crystal can be grown (Viviani and Golia, 2003; Eyer and Leiste, 1985; Doi and Koster, 1993; Li *et al*., 2002; Li *et al*., 2006).

In the absence of body forces, long liquid capillary bridges are normally unstable because of the growth of a mode where one end becomes slender while the other becomes rotund. This so-called Rayleigh-Plateau (RP) instability was suppressed for

weightless bridges on NASA's KC-135 aircraft by placing the bridge in an acoustic standing wave (Thiessen *et al*., 2002). In addition to liquid bridges, RP instability is relevant to the breakup of liquid jets and coatings, and to the dynamics of drops and bubbles (Moseler and Landman, 2000). Marr-Lyon *et al*.(1997; 2000) investigated the response of liquid bridges to acoustic radiation pressure, and demonstrated that active control of normal stresses at the liquid surface can suppress the RP instability for bridges significantly beyond the RP limit using either acoustic or electrostatic stresses. Subsequently, Marr-Lyon *et al*.(2001) explored the possibility of countering this instability for a liquid bridge in air and a cylindrical bubble of air in water, through a novel passive stabilization effect of an appropriately chosen sound field in which the bridge is immersed. For a recent review on the subject, the reader is referred to the work by Wei *et al*.(2004) who considered an infinitely long fluid cylinder in an acoustic plane standing wave field and obtained a simple long wavelength approximation of the radiation force-per-length for the following situations: a hot gas column, a compressible liquid bridge in a Plateau tank, a liquid bridge in air, and a cylindrical bubble of air in water.

In this paper we employ the translation addition theorem for cylindrical Bessel functions to study scattering of compressional acoustic waves by an eccentrically coated thermovisous fluid cylinder submerged in a boundless viscous thermally conducting fluid medium. Particular emphasis is put on assessment of eccentricity as well as thermoviscous loss effects. The proposed model is of notable interest essentially due to its inherent value as a canonical problem in general acoustics. It can form an invaluable guide in establishing the thresholds for influence of eccentricity and thermoviscosity in terms of the incident wave field characteristics. The presented exact solution can serve as the benchmark for comparison to other solutions obtained by strictly numerical or asymptotic approaches. It has promising applications in a wide range of physical and technical fields including detection and characterization of internal structure of compound bodies (Sinai and Waag, 1988), and passive acoustic stabilization and breakup control of fluid-encapsulated liquid bridges, small diffusion flames and hot cylindrical fluid objects under microgravity conditions (Wei *et al*., 2004; Marr-Lyon *et al*., 1997; 2000; 2001; Johnson, 2002; Viviani and Golia, 2003; Li *et al*., 2002).

FORMULATION

Basic model

There are a seemingly endless variety of models available now dealing with thermoviscous effects in acoustic wave propagation. The most exclusive model is based on a solution of the full set of basic governing equations, i.e., all terms in the linearized Navier Stokes equations are taken into account. This inclusive treatment of thermoviscosity can greatly complicate the analysis because the fluid medium can then support shear and thermal as well as compressional modes, both of which must be accounted for in satisfying the boundary conditions at the interfaces. Here, we theoretically examine the 2D scattered acoustic field produced by an incident plane wave on a compound fluid cylinder defined by two nonconcentric cylindrical surfaces of radii a and b. The cylinder axes extend to infinity and are parallel. The cylinder is thermoviscous and is immersed in another (a boundless) thermoviscous fluid medium. The incident wave direction of propagation is normal to its axis. The problem geometry is shown in Fig.1. Two cylindrical coordinate systems are introduced to describe the different acoustic fields inside and outside the compound cylinder. Their origin-to-origin separation is e, and point P is an arbitrary field point outside the fluid cylinder.

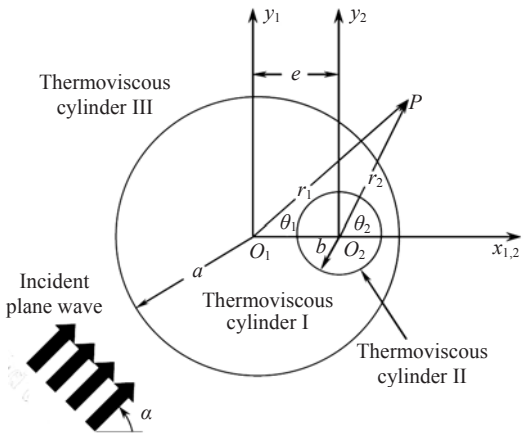

Fig.1 Problem geometry

The classical Helmholtz decomposition expansion may advantageously be employed to express fluid-particle velocity vector in the thermoviscous acoustic medium in terms of a compressional-wave scalar potential and a viscous-wave vector potential as

$$\boldsymbol{u} = -\nabla\varphi + \nabla\times\boldsymbol{\psi}\,. \tag{1}$$

The governing equations for φ, $\boldsymbol{\psi}$ and the excess temperature T is then written as (Temkin, 1981):

$$\begin{cases} -\omega^2\varphi + \mathrm{i}\omega\eta\, c^2 T/\gamma = (c^2/\gamma - \mathrm{i}\omega\beta)\nabla^2\varphi, \\ -\mathrm{i}\omega T = \kappa\nabla^2 T/(\rho C_\mathrm{v}) + (\gamma-1)\nabla^2\varphi/\eta, \\ -\mathrm{i}\omega\boldsymbol{\psi} = \nu\nabla^2\boldsymbol{\psi}, \end{cases} \tag{2}$$

where κ is the thermal conductivity, C_v is the specific heat at constant volume, ρ is the mass density, $\beta=4\nu/3+\mu_\mathrm{b}/\rho$, $\nu=\mu/\rho$ is the kinematic viscosity, μ is shear (dynamic) viscosity, μ_b is the bulk (expansive) viscosity, c is the adiabatic speed of sound, η is the coefficient of thermal expansion, $\gamma=C_\mathrm{p}/C_\mathrm{v}$ is the specific heat ratio and C_p is the specific heat at constant pressure. Also, in view of the fact that the incident wave is time-harmonic, with the circular frequency ω, we have assumed harmonic time variations throughout with the $\mathrm{e}^{-\mathrm{i}\omega t}$ dependence suppressed for simplicity. The above governing equations may be algebraically manipulated to yield Helmholtz-type equations (Temkin, 1981):

$$\begin{cases} (\nabla^2 + k_\mathrm{c}^2)\phi_\mathrm{c} = 0, \\ (\nabla^2 + k_\mathrm{t}^2)\phi_\mathrm{t} = 0, \\ (\nabla^2 + k_\mathrm{s}^2)\boldsymbol{\psi} = 0, \end{cases} \tag{3}$$

where the subscripts 'c', 't' and 's' denote compressional, thermal and shear, respectively. In addition, $\varphi=\varphi_\mathrm{c}+\varphi_\mathrm{t}$, and accurate approximations for k_c, k_t and k_s are given as:

$$\begin{cases} k_\mathrm{c} = \dfrac{\omega}{c}\left[1+\mathrm{i}\dfrac{\omega\nu}{2c^2}\left(\dfrac{4}{3}+\dfrac{\mu_\mathrm{b}}{\mu}+\dfrac{\gamma-1}{Pr}\right)\right], \\ k_\mathrm{t} = (1+\mathrm{i})\sqrt{\omega/(2\sigma)}, \\ k_\mathrm{s} = (1+\mathrm{i})\sqrt{\omega/(2\nu)}, \end{cases} \tag{4}$$

where $Pr=\mu C_\mathrm{p}/\kappa$ is Prandtl number and $\sigma=\kappa/(\rho C_\mathrm{p})$ is the thermal diffusivity. Making use of problem symmetry, $\boldsymbol{\psi}=(0,0,\psi)$ and ∇ is classical. Therefore, Eq.(1) yields for the radial and tangential velocities, and with $\varphi=\varphi_\mathrm{c}+\varphi_\mathrm{t}$, the first of Eq.(2) and the first two of Eq.(3) yield for the excess temperature (Hasheminejad and Geers, 1993):

$$\begin{cases} u_r = -\dfrac{\partial\varphi}{\partial r} + \dfrac{1}{r}\dfrac{\partial\psi}{\partial\theta}, \\ u_\theta = -\dfrac{1}{r}\dfrac{\partial\varphi}{\partial\theta} - \dfrac{\partial\psi}{\partial r}, \\ T = b_\mathrm{c}\varphi_\mathrm{c} + b_\mathrm{t}\varphi_\mathrm{t}, \end{cases} \tag{5}$$

where

$$\begin{cases} b_\mathrm{c} = \dfrac{\gamma}{\mathrm{i}\omega\eta c^2}\left[\omega^2 - k_\mathrm{c}^2(c^2/\gamma - \mathrm{i}\omega\beta)\right], \\ b_\mathrm{t} = \dfrac{\gamma}{\mathrm{i}\omega\eta c^2}\left[\omega^2 - k_\mathrm{t}^2(c^2/\gamma - \mathrm{i}\omega\beta)\right]. \end{cases} \tag{6}$$

In addition, the classical relations for radial and tangential stresses, heat flux, and acoustic pressure may be employed to yield the following potential-based expressions (Lin and Raptis, 1983):

$$\begin{cases} \sigma_{rr} \\ = -p - \left(\mu_\mathrm{b} - \dfrac{2}{3}\mu\right)\nabla^2\varphi - 2\mu\left(\dfrac{\partial^2\varphi}{\partial r^2} + \dfrac{1}{r^2}\dfrac{\partial\psi}{\partial\theta} - \dfrac{1}{r}\dfrac{\partial^2\psi}{\partial r\,\partial\theta}\right), \\ \sigma_{r\theta} \\ = \mu\left(-\dfrac{2}{r}\dfrac{\partial^2\varphi}{\partial r\,\partial\theta} + \dfrac{2}{r^2}\dfrac{\partial\varphi}{\partial\theta} + \dfrac{1}{r^2}\dfrac{\partial^2\psi}{\partial\theta^2} + \dfrac{1}{r}\dfrac{\partial\psi}{\partial r} - \dfrac{\partial^2\psi}{\partial r^2}\right), \\ q = -\kappa\left(b_\mathrm{c}\dfrac{\partial\varphi_\mathrm{c}}{\partial r} + b_\mathrm{t}\dfrac{\partial\varphi_\mathrm{t}}{\partial r}\right), \end{cases} \tag{7}$$

where

$$p = -\mathrm{i}\,\omega\rho\varphi - \left(\mu_\mathrm{b} + \frac{4}{3}\mu\right)\nabla^2\varphi. \tag{8}$$

Field expansions and boundary conditions

Following the standard methods in theoretical acoustics, the dynamics of the problem may be expressed in terms of appropriate scalar potentials. The thermoviscous fluid coating is represented by region I, while the cylindrical fluid core is denoted as region II

and the boundless thermoviscous fluid medium is denoted as region III (Fig.1). The incident wave in the surrounding thermoviscous fluid (medium III) with respect to the first coordinate system may be written in the form (Lin and Raptis, 1983):

$$\varphi_{\text{inc}} = \varphi_0 \sum_{n=-\infty}^{\infty} \mathrm{i}^n J_n(kr_1)\exp[\mathrm{i}n(\theta_1-\alpha)], \qquad (9)$$

in which J_n is the cylindrical Bessel function of the first kind (Abramowitz and Stegun, 1965), φ_0 is the amplitude of the incident wave, k=Re(k_{c3}) and α is the angle of incidence.

In region III, the possibility of outgoing waves exists, while in region I, the possibility of both incoming and outgoing (standing) waves exists. Furthermore, in region II only incoming waves are possible. Therefore, the solution of the Helmholtz equations for the acoustic velocity potentials in the ambient thermoviscous fluid medium may be as follows:

$$\begin{cases} \varphi_{\text{c}}^{\text{III}}(r_1,\theta_1,\omega) = \sum_{n=-\infty}^{\infty} A_n(\omega)H_n(k_{\text{c3}}r_1)\exp(\mathrm{i}n\theta_1), \\ \varphi_{\text{t}}^{\text{III}}(r_1,\theta_1,\omega) = \sum_{n=-\infty}^{\infty} B_n(\omega)H_n(k_{\text{t3}}r_1)\exp(\mathrm{i}n\theta_1), \\ \psi^{\text{III}}(r_1,\theta_1,\omega) = \sum_{n=-\infty}^{\infty} C_n(\omega)H_n(k_{\text{s3}}r_1)\exp(\mathrm{i}n\theta_1), \end{cases} \qquad (10)$$

where, $H_n(x)=J_n(x)+\mathrm{i}Y_n(x)$ is the cylindrical Hankel function of the first kind (Abramowitz and Stegun, 1965), and $A_n(\omega)$, $B_n(\omega)$ and $C_n(\omega)$ are unknown scattering coefficients. Similarly, the solution of the Helmholtz equations for the acoustic velocity potentials inside the thermoviscous fluid coating may be represented by (Hasheminejad and Azarpeyvand, 2003):

$$\begin{cases} \varphi_{\text{c}}^{\text{I}} = \sum_{n=-\infty}^{\infty} \{D_n(\omega)J_n(k_{\text{c1}}r_1)\exp(\mathrm{i}n\theta_1) \\ \qquad + E_n(\omega)H_n(k_{\text{c1}}r_2)\exp(\mathrm{i}n\theta_2)\}, \\ \varphi_{\text{t}}^{\text{I}} = \sum_{n=-\infty}^{\infty} \{F_n(\omega)J_n(k_{\text{t1}}r_1)\exp(\mathrm{i}n\theta_1) \\ \qquad + G_n(\omega)H_n(k_{\text{t1}}r_2)\exp(\mathrm{i}n\theta_2)\}, \\ \psi^{\text{I}} = \sum_{n=-\infty}^{\infty} \{K_n(\omega)J_n(k_{\text{s1}}r_1)\exp(\mathrm{i}n\theta_1) \\ \qquad + L_n(\omega)H_n(k_{\text{s1}}r_2)\exp(\mathrm{i}n\theta_2)\}. \end{cases} \qquad (11)$$

We note that in the above equations, the last (first) terms are expressed in the second (first) coordinate systems. These terms have to be transformed to the first (second) coordinate system before imposing the boundary conditions. Also, the acoustic velocity potentials inside the cylindrical fluid core may be represented by:

$$\begin{cases} \varphi_{\text{c}}^{\text{II}}(r_2,\theta_2,\omega) = \sum_{n=-\infty}^{\infty} P_n(\omega)J_n(k_{\text{c2}}r_2)\exp(\mathrm{i}n\theta_2), \\ \varphi_{\text{t}}^{\text{II}}(r_2,\theta_2,\omega) = \sum_{n=-\infty}^{\infty} Q_n(\omega)J_n(k_{\text{t2}}r_2)\exp(\mathrm{i}n\theta_2), \\ \psi^{\text{II}}(r_2,\theta_2,\omega) = \sum_{n=-\infty}^{\infty} R_n(\omega)J_n(k_{\text{s2}}r_2)\exp(\mathrm{i}n\theta_2). \end{cases} \qquad (12)$$

The unknown scattering coefficients $A_n(\omega)$ through $R_n(\omega)$ must be determined by imposing the suitable boundary conditions. Accordingly, the continuity of the normal and tangential velocity components, temperature, heat flux and the normal and tangential stresses at the inner and outer surfaces of the cylindrical fluid coating demand that (Hasheminejad and Geers, 1993)

$$\begin{aligned} &u_r^{\text{I}}\big|_{r_1=a} = u_r^{\text{III}}\big|_{r_1=a},\ \sigma_{rr}^{\text{I}}\big|_{r_1=a} = \sigma_{rr}^{\text{III}}\big|_{r_1=a},\ T^{\text{I}}\big|_{r_1=a} = T^{\text{III}}\big|_{r_1=a}; \\ &u_\theta^{\text{I}}\big|_{r_1=a} = u_\theta^{\text{III}}\big|_{r_1=a},\ \sigma_{r\theta}^{\text{I}}\big|_{r_1=a} = \sigma_{r\theta}^{\text{III}}\big|_{r_1=a},\ q^{\text{I}}\big|_{r_1=a} = q^{\text{III}}\big|_{r_1=a}; \\ &u_r^{\text{I}}\big|_{r_2=b} = u_r^{\text{II}}\big|_{r_2=b},\ \sigma_{rr}^{\text{I}}\big|_{r_2=b} = \sigma_{rr}^{\text{II}}\big|_{r_2=b},\ T^{\text{I}}\big|_{r_2=b} = T^{\text{II}}\big|_{r_2=b}; \\ &u_\theta^{\text{I}}\big|_{r_2=b} = u_\theta^{\text{II}}\big|_{r_2=b},\ \sigma_{r\theta}^{\text{I}}\big|_{r_2=b} = \sigma_{r\theta}^{\text{II}}\big|_{r_2=b},\ q^{\text{I}}\big|_{r_2=b} = q^{\text{II}}\big|_{r_2=b}. \end{aligned} \qquad (13)$$

Wave transformations and series representations

Many radiation and scattering problems involve waves of one characteristic shape (coordinate system) that are incident upon a boundary of some other shapes (coordinate system). So it is difficult to satisfy the boundary conditions on that surface. There exists, however, a class of mathematical relationships called wave transformations that circumvent this difficulty in many cases by allowing one to study the fields scattered by the various bodies (interfaces), all referred to a common origin. Accordingly, to fulfill orthogonality in the current problem, we need to express the cylindrical wave functions of the first (second) coordinate system in terms of cylindrical wave functions of the second (first) coordinate system

by application of the classical form of translational addition theorem for cylindrical coordinates (Stratton, 1941):

$$\begin{cases} H_n(k^*r_2)\exp(\mathrm{i}n\theta_2) \\ \quad = \sum\limits_{m=-\infty}^{\infty} J_{m-n}(k^*e)H_m(k^*r_1)\exp(\mathrm{i}m\theta_1), \\ J_n(k^*r_1)\exp(\mathrm{i}n\theta_1) \\ \quad = \sum\limits_{m=-\infty}^{\infty} J_{n-m}(k^*e)J_m(k^*r_2)\exp(\mathrm{i}m\theta_2), \end{cases} \tag{14}$$

where k^* can be any of k_{c1}, k_{t1} or k_{s1}. Subsequently, the above addition theorem may be utilized in Eq.(11) to express the acoustic field potentials in the fluid coating (region I) with respect to the first or second coordinate system, i.e.,

$$\begin{cases} \varphi_c^{\mathrm{I}}(r_1,\theta_1,\omega) = \sum\limits_{n=-\infty}^{\infty} D_n(\omega)J_n(k_{c1}r_1)\exp(\mathrm{i}n\theta_1) \\ \qquad + \sum\limits_{n=-\infty}^{\infty} E_{nm}^*(\omega)H_n(k_{c1}r_1)\exp(\mathrm{i}n\theta_1), \\ \varphi_t^{\mathrm{I}}(r_1,\theta_1,\omega) = \sum\limits_{n=-\infty}^{\infty} F_n(\omega)J_n(k_{t1}r_1)\exp(\mathrm{i}n\theta_1) \\ \qquad + \sum\limits_{n=-\infty}^{\infty} G_{nm}^*(\omega)H_n(k_{t1}r_1)\exp(\mathrm{i}n\theta_1), \\ \psi^{\mathrm{I}}(r_1,\theta_1,\omega) = \sum\limits_{n=-\infty}^{\infty} K_n(\omega)J_n(k_{s1}r_1)\exp(\mathrm{i}n\theta_1) \\ \qquad + \sum\limits_{n=-\infty}^{\infty} L_{nm}^*(\omega)H_n(k_{s1}r_1)\exp(\mathrm{i}n\theta_1), \end{cases} \tag{15}$$

or

$$\begin{cases} \varphi_c^{\mathrm{I}}(r_2,\theta_2,\omega) = \sum\limits_{n=-\infty}^{\infty} D_{nm}^*(\omega)J_n(k_{c1}r_2)\exp(\mathrm{i}n\theta_2) \\ \qquad + \sum\limits_{n=-\infty}^{\infty} E_n(\omega)H_n(k_{c1}r_2)\exp(\mathrm{i}n\theta_2), \\ \varphi_t^{\mathrm{I}}(r_2,\theta_2,\omega) = \sum\limits_{n=-\infty}^{\infty} F_{nm}^*(\omega)J_n(k_{t1}r_2)\exp(\mathrm{i}n\theta_2) \\ \qquad + \sum\limits_{n=-\infty}^{\infty} G_n(\omega)H_n(k_{t1}r_2)\exp(\mathrm{i}n\theta_2), \\ \psi^{\mathrm{I}}(r_2,\theta_2,\omega) = \sum\limits_{n=-\infty}^{\infty} K_{nm}^*(\omega)J_n(k_{s1}r_2)\exp(\mathrm{i}n\theta_2) \\ \qquad + \sum\limits_{n=-\infty}^{\infty} L_n(\omega)H_n(k_{s1}r_2)\exp(\mathrm{i}n\theta_2), \end{cases} \tag{16}$$

where

$$\begin{cases} D_{nm}^*(\omega) = \sum\limits_{m=-\infty}^{\infty} D_m(\omega)J_{m-n}(k_{c1}e), \\ E_{nm}^*(\omega) = \sum\limits_{m=-\infty}^{\infty} E_m(\omega)J_{n-m}(k_{c1}e), \\ F_{nm}^*(\omega) = \sum\limits_{m=-\infty}^{\infty} F_m(\omega)J_{m-n}(k_{t1}e), \\ G_{nm}^*(\omega) = \sum\limits_{m=-\infty}^{\infty} G_m(\omega)J_{n-m}(k_{t1}e), \\ K_{nm}^*(\omega) = \sum\limits_{m=-\infty}^{\infty} K_m(\omega)J_{m-n}(k_{s1}e), \\ L_{nm}^*(\omega) = \sum\limits_{m=-\infty}^{\infty} L_m(\omega)J_{n-m}(k_{s1}e). \end{cases} \tag{17}$$

Now utilization of Eqs.(9), (10), (12), (15) and (16) in the boundary conditions Eq.(13) yields

$$\begin{aligned} &-k_{c3}H_n'(k_{c3}a)A_n - k_{t3}H_n'(k_{t3}a)B_n + (\mathrm{i}n/a)H_n(k_{s3}a)C_n \\ &+k_{c1}J_n'(k_{c1}a)D_n + k_{c1}H_n'(k_{c1}a)E_{nm}^* + k_{t1}J_n'(k_{t1}a)F_n \\ &+k_{t1}H_n'(k_{t1}a)G_{nm}^* - (\mathrm{i}n/a)J_n(k_{s1}a)K_n \\ &-(\mathrm{i}n/a)H_n(k_{s1}a)L_{nm}^* = \varphi_0 k\mathrm{i}^n\exp(-\mathrm{i}n\alpha)J_n'(ka), \end{aligned} \tag{18}$$

$$\begin{aligned} &-(\mathrm{i}n/a)H_n(k_{c3}a)A_n - (\mathrm{i}n/a)H_n(k_{t3}a)B_n \\ &-k_{s3}H_n'(k_{s3}a)C_n + (\mathrm{i}n/a)J_n(k_{c1}a)D_n \\ &+(\mathrm{i}n/a)H_n(k_{c1}a)E_{nm}^* + (\mathrm{i}n/a)J_n(k_{t1}a)F_n \\ &+(\mathrm{i}n/a)H_n(k_{t1}a)G_{nm}^* + k_{s1}J_n'(k_{s1}a)K_n \\ &+k_{s1}H_n'(k_{s1}a)L_{nm}^* \\ &= \varphi_0(n/a)\mathrm{i}^{n+1}\exp(-\mathrm{i}n\alpha)J_n(ka), \end{aligned} \tag{19}$$

$$\begin{aligned} &\left\{(\mathrm{i}\omega\rho_3 - 2\mu_3k_{c3}^2)H_n(k_{c3}a) - 2\mu_3k_{c3}^2H_n''(k_{c3}a)\right\}A_n \\ &+\left\{(\mathrm{i}\omega\rho_3 - 2\mu_3k_{t3}^2)H_n(k_{t3}a) - 2\mu_3k_{t3}^2H_n''(k_{t3}a)\right\}B_n \\ &+2\mu_3\mathrm{i}(n/a^2)\left\{ak_{s3}H_n'(k_{s3}a) - H_n(k_{s3}a)\right\}C_n \\ &-\left\{(\mathrm{i}\omega\rho_1 - 2\mu_1k_{c1}^2)J_n(k_{c1}a) - 2\mu_1k_{c1}^2J_n''(k_{c1}a)\right\}D_n \\ &-\left\{(\mathrm{i}\omega\rho_1 - 2\mu_1k_{c1}^2)H_n(k_{c1}a) - 2\mu_1k_{c1}^2H_n''(k_{c1}a)\right\}E_{nm}^* \\ &-\left\{(\mathrm{i}\omega\rho_1 - 2\mu_1k_{t1}^2)J_n(k_{t1}a) - 2\mu_1k_{t1}^2J_n''(k_{t1}a)\right\}F_n \\ &-\left\{(\mathrm{i}\omega\rho_1 - 2\mu_1k_{t1}^2)H_n(k_{t1}a) - 2\mu_1k_{t1}^2H_n''(k_{t1}a)\right\}G_{nm}^* \\ &-2\mu_1\mathrm{i}(n/a^2)\left\{ak_{s1}J_n'(k_{s1}a) - J_n(k_{s1}a)\right\}K_n \\ &-2\mu_1\mathrm{i}(n/a^2)\left\{ak_{s1}H_n'(k_{s1}a) - H_n(k_{s1}a)\right\}L_{nm}^* \\ &= \varphi_0\mathrm{i}^n\exp(-\mathrm{i}n\alpha)\left\{(2\mu_3k^2 - \mathrm{i}\omega\rho_3)J_n(ka) + 2\mu_3k^2J_n''(ka)\right\}, \end{aligned} \tag{20}$$

$$2\mu_3\mathrm{i}(n/a^2)\left\{-ak_{c3}H_n'(k_{c3}a) + H_n(k_{c3}a)\right\}A_n$$

$$+2\mu_3\mathrm{i}(n/a^2)\{-ak_{t3}H_n'(k_{t3}a)+H_n(k_{t3}a)\}B_n$$
$$+\{-\mu_3(n^2/a^2)H_n(k_{s3}a)+k_{s3}(\mu_3/a)H_n'(k_{s3}a)$$
$$-\mu_3k_{s3}^2H_n''(k_{s3}a)\}C_n+2\mu_1\mathrm{i}(n/a^2)\{ak_{c1}J_n'(k_{c1}a)$$
$$-J_n(k_{c1}a)\}D_n+2\mu_1\mathrm{i}(n/a^2)\{ak_{t1}H_n'(k_{c1}a)-H_n(k_{c1}a)\}E_{nm}^*$$
$$+2\mu_1\mathrm{i}(n/a^2)\{ak_{t1}J_n'(k_{t1}a)-J_n(k_{t1}a)\}F_n$$
$$+2\mu_1\mathrm{i}(n/a^2)\{ak_{t1}H_n'(k_{t1}a)-H_n(k_{t1}a)\}G_{nm}^*$$
$$+(\mu_1/a^2)\{n^2J_n(k_{s1}a)-k_{s1}aJ_n'(k_{s1}a)+a^2k_{s1}^2J_n''(k_{s1}a)\}K_n$$
$$+(\mu_1/a^2)\{n^2H_n(k_{s1}a)-k_{s1}aH_n'(k_{s1}a)+a^2k_{s1}^2H_n''(k_{s1}a)\}L_{nm}^*$$
$$=2\varphi_0\mu_3\mathrm{i}^{n+1}\exp(-\mathrm{i}n\alpha)(n/a^2)\{\mathrm{a}kJ_n'(ka)-J_n(ka)\}, \quad (21)$$

$$B_{c3}H_n(k_{c3}a)A_n+B_{t3}H_n(k_{t3}a)B_n-B_{c1}J_n(k_{c1}a)D_n$$
$$-B_{c1}H_n(k_{c1}a)E_{nm}^*-B_{t1}J_n(k_{t1}a)F_n-B_{t1}H_n(k_{t1}a)G_{nm}^*$$
$$=-\varphi_0\mathrm{i}^n\exp(-\mathrm{i}n\alpha)B_{c3}J_n(ka), \quad (22)$$

$$-\kappa_3B_{c3}k_{c3}H_n'(k_{c3}a)A_n-\kappa_3B_{t3}k_{t3}H_n'(k_{t3}a)B_n$$
$$+\kappa_1B_{c1}k_{c1}J_n'(k_{c1}a)D_n+\kappa_1B_{c1}k_{c1}H_n'(k_{c1}a)E_{nm}^*$$
$$+\kappa_1B_{t1}k_{t1}J_n'(k_{t1}a)F_n+\kappa_1B_{t1}k_{t1}H_n'(k_{t1}a)G_{nm}^*$$
$$=\varphi_0\mathrm{i}^n\exp(-\mathrm{i}n\alpha)\kappa_3B_{c3}kJ_n'(ka), \quad (23)$$

$$-k_{c1}J_n'(k_{c1}b)D_{nm}^*-k_{c1}H_n'(k_{c1}b)E_n-k_{t1}J_n'(k_{t1}b)F_{nm}^*$$
$$-k_{t1}H_n'(k_{t1}b)G_n+(\mathrm{i}n/b)J_n(k_{s1}b)K_{nm}^*+(\mathrm{i}n/b)H_n(k_{s1}b)L_n$$
$$+k_{c2}J_n'(k_{c2}b)P_n+k_{t2}J_n'(k_{t2}b)Q_n-(\mathrm{i}n/b)J_n(k_{s2}b)R_n=0, \quad (24)$$

$$-(\mathrm{i}n/b)J_n(k_{c1}b)D_{nm}^*-(\mathrm{i}n/b)H_n(k_{c1}b)E_n$$
$$-(\mathrm{i}n/b)J_n(k_{t1}b)F_{nm}^*-(\mathrm{i}n/b)H_n(k_{t1}b)G_n$$
$$-k_{s1}J_n'(k_{s1}b)K_{nm}^*-k_{s1}H_n'(k_{s1}b)L_n+(\mathrm{i}n/b)J_n(k_{c2}b)P_n$$
$$+(\mathrm{i}n/b)J_n(k_{t2}b)Q_n+k_{s2}J_n'(k_{s2}b)R_n=0, \quad (25)$$

$$\{(\mathrm{i}\omega\rho_1-2\mu_1k_{c1}^2)J_n(k_{c1}b)-2\mu_1k_{c1}^2J_n''(k_{c1}b)\}D_{nm}^*$$
$$+\{(\mathrm{i}\omega\rho_1-2\mu_1k_{c1}^2)H_n(k_{c1}b)-2\mu_1k_{c1}^2H_n''(k_{c1}b)\}E_n$$
$$+\{(\mathrm{i}\omega\rho_1-2\mu_1k_{t1}^2)J_n(k_{t1}b)-2\mu_1k_{t1}^2J_n''(k_{t1}b)\}F_{nm}^*$$
$$+\{(\mathrm{i}\omega\rho_1-2\mu_1k_{t1}^2)H_n(k_{t1}b)-2\mu_1k_{t1}^2H_n''(k_{t1}b)\}G_n$$
$$+2\mu_1\mathrm{i}(n/b^2)\{bk_{s1}J_n'(k_{s1}b)-J_n(k_{s1}b)\}K_{nm}^*$$
$$+2\mu_1\mathrm{i}(n/b^2)\{bk_{s1}H_n'(k_{s1}b)-H_n(k_{s1}b)\}L_n$$
$$-\{(\mathrm{i}\omega\rho_2-2\mu_2k_{c2}^2)J_n(k_{c2}b)-2\mu_2k_{c2}^2J_n''(k_{c2}b)\}P_n$$
$$-\{(\mathrm{i}\omega\rho_2-2\mu_2k_{t2}^2)J_n(k_{t2}b)-2\mu_2k_{t2}^2J_n''(k_{t2}b)\}Q_n$$
$$-2\mu_2\mathrm{i}(n/b^2)\{bk_{s2}J_n'(k_{s2}b)-J_n(k_{s2}b)\}R_n=0, \quad (26)$$

$$2\mu_1\mathrm{i}(n/b^2)\{J_n(k_{c1}b)-bk_{c1}J_n'(k_{c1}b)\}D_{nm}^*$$
$$+2\mu_1\mathrm{i}(n/b^2)\{-bk_{c1}H_n'(k_{c1}b)+H_n(k_{c1}b)\}E_n$$
$$+2\mu_1\mathrm{i}(n/b^2)\{J_n(k_{t1}b)-bk_{t1}J_n'(k_{t1}b)\}F_{nm}^*$$
$$+2\mu_1\mathrm{i}(n/b^2)\{-bk_{t1}H_n'(k_{t1}b)+H_n(k_{t1}b)\}G_n$$
$$+\{-\mu_1(n^2/b^2)J_n(k_{s1}b)+k_{s1}(\mu_1/b)J_n'(k_{s1}b)$$
$$-\mu_1k_{s1}^2J_n''(k_{s1}b)\}K_{nm}^*+\{-\mu_1(n^2/b^2)H_n(k_{s1}b)$$
$$+k_{s1}(\mu_1/b)H_n'(k_{s1}b)-\mu_1k_{s1}^2H_n''(k_{s1}b)\}L_n$$
$$+2\mu_2\mathrm{i}(n/b^2)\{bk_{c2}J_n'(k_{c1}b)-J_n(k_{c2}b)\}P_n$$
$$+2\mu_2\mathrm{i}(n/b^2)\{bk_{t2}J_n'(k_{t2}b)-J_n(k_{t2}b)\}Q_n$$
$$+\{\mu_2(n^2/b^2)J_n(k_{s2}b)-k_{s2}(\mu_2/b)J_n'(k_{s2}b)$$
$$+\mu_2k_{s2}^2J_n''(k_{s2}b)\}R_n=0, \quad (27)$$

$$B_{c1}J_n(k_{c1}b)D_{nm}^*+B_{c1}H_n(k_{c1}b)E_n+B_{t1}J_n(k_{t1}b)F_{nm}^*$$
$$+B_{t1}H_n(k_{t1}b)G_n-B_{c2}J_n(k_{c2}b)P_n-B_{t2}J_n(k_{t2}b)Q_n=0, \quad (28)$$

$$\kappa_1B_{c1}k_{c1}J_n'(k_{c1}b)D_{nm}^*+\kappa_1B_{c1}k_{c1}H_n'(k_{c1}b)E_n$$
$$+\kappa_1B_{t1}k_{t1}J_n'(k_{t1}b)F_{nm}^*+\kappa_1B_{t1}k_{t1}H_n'(k_{t1}b)G_n$$
$$-\kappa_2B_{c2}k_{c2}J_n'(k_{c2}b)P_n-\kappa_2B_{t2}k_{t2}J_n'(k_{t2}b)Q_n=0. \quad (29)$$

This completes the necessary background required for the exact acoustic scattering analysis of a fluid-encapsulated thermoviscous fluid cylinder. Next we consider some numerical examples.

NUMERICAL RESULTS

In order to illustrate the natural and general behaviour of the solution, we consider some numerical examples in this section. Realizing the crowd of parameters and the intense computations involved here, no attempt is made to exhaustively evaluate the effect of varying each of them. Thus, we confine our attention to a particular model. The surrounding ambient fluid is assumed to be glycerine at atmospheric pressure and 300 K. The fluid cylinder (a=0.1 cm) is supposed to be made from 3M "Fluorinert" chemical FC-75 (http://www.mmm.com) and the core fluid (b=0.1a, 0.5a) is selected to be olive oil (Babick *et al*., 2000), with their physical properties summarized in Table 1. A FORTRAN code was constructed for treating boundary conditions and to calculate the unknown scattering coefficients and the relevant acoustic field quantities as functions of the nondimensional frequency ka, the angle of plane wave incidence α, the dimensionless eccentricity and radii ratio parameters e/a and b/a. Accurate computations

Table 1 The input parameter values used in calculations

Parameter	FC-75 (Medium I)	Olive oil (Medium II)	Glycerine (Medium III)
μ [kg/(m·s)]	0.0079	0.84	9.5
μ_b [kg/(m·s)]	0.0079	0.84	9.5
c (m/s)	613.7	1440	1910
κ [N/(s·K)]	0.0639	0.19	0.286
η (K^{-1})	1.799×10^{-3}	7.2×10^{-4}	6.1×10^{-4}
C_p [J/(kg·K)]	1044	2000	2427
C_v [J/(kg·K)]	1038	2000	2427
ρ (kg/m^3)	1730	900	1250

of cylindrical Bessel functions of complex arguments and their derivatives were accomplished by utilizing the module CH12N described in the monograph by Zhang and Jin (1996). The precision of calculated values was checked against Maple specialized math functions "*HankelH1*" and "*BesselJ*", and also the printed tabulations in the handbook by Abramowitz and Stegun (1965). Matrix inversions were carried out using the subroutine ZGEFA from the portable numerical software library LINPAK (Dongarra *et al*., 1979). The computations were performed on a Pentium IV personal computer with truncation constants of n_{max}=m_{max}=35 to assure convergence in the high frequency/eccentricity range. In addition to avoid numerical overflow/underflow problems at high frequencies (i.e., for large complex arguments), an extension of the range of the floating point numbers was pursued. This enables us to make computation using numeric precision beyond the single or double precision ordinarily provided in hardware. Accordingly, a very powerful multi-precision FORTRAN software package MPFUN developed by Bailey (1995) from NASA was employed to compute mathematical functions on floating point numbers of arbitrarily high precision.

The primary acoustic field quantities are the far-field backscattered pressure amplitude and the total acoustic pressure distribution. Using Eq.(3) in Eq.(8), the backscattered and the total acoustic pressure amplitudes with respect to the first coordinate system are respectively written as:

$$\begin{aligned}\left|p_{\text{scat}}(r_1,\theta_1=\alpha+\pi,\omega)\right| &= \left|-\mathrm{i}\omega\rho_3(\varphi_c^{\text{III}}+\varphi_t^{\text{III}})\right.\\ &\left.+(\mu_{b3}+4\mu_3/3)\left[k_{c3}^2\varphi_c^{\text{III}}+k_{t3}^2\varphi_t^{\text{III}}\right]\right|,\\ \left|p(r_1,\theta_1,\omega)\right| &= \left|-\mathrm{i}\omega\rho_3(\varphi_{\text{inc}}+\varphi_c^{\text{III}}+\varphi_t^{\text{III}})\right.\\ &\left.+(\mu_{b3}+4\mu_3/3)\left[k_{c3}^2(\varphi_{\text{inc}}+\varphi_c^{\text{III}})+k_{t3}^2\varphi_t^{\text{III}}\right]\right|.\end{aligned} \tag{30}$$

The two most important incidence angles are α=0 (end-on) and α=π/2 (broadside), as they best help to expose the physics of the problem. Figs.2a and 2b display the variation of the normalized backscattered acoustic pressure magnitude, $|p_{\text{scat}}(r_1,\ \theta_1=\alpha+\pi,\ \omega)|/(\omega\rho_3\varphi_0)$, with ka for a unit amplitude plane wave (φ_0=1) at a far-field point (r_1=50a) for broadside/end-on incidence at selected eccentricities and inclusion sizes (b/a=0.1, 0.5). We have also generated the normalized backscatted far-field pressure amplitude curves for a compound ideal fluid cylinder (solid line) by using an independently developed FORTRAN code. The main observations are as follows. At very low to intermediate incident wave frequencies (0<ka<3), the thermoviscous effects are very insignificant, as the solid and dotted lines almost entirely coincide. Thermoviscosity has an increasingly depressing effect on the pressure amplitudes starting at intermediate frequencies (ka>3). At the highest incident wave frequency (ka=10), inclusion of thermoviscous effects leads to a substantial decrease in the overall pressure magnitudes almost regardless of inclusion size, eccentricity or angle of incidence. As the eccentricity parameter (e/a) is increased, the themoviscous effects appear to increase, more rapidly in the end-on incidence (α=0) situation. In fact, the largest damping occurs at the highest frequency ($k\alpha$=10) for biggest eccentricity in the end-on incidence (α=0) case for both inclusion sizes. Furthermore, the backscattered pressure peaks become more densely packed as the eccentricity grows, especially at high frequencies in the end-on incidence (α=0) case. This behaviour is principally caused by interference of the fields scattered by the two eccentric cylindrical boundaries. More specifically, it is associated with the fact that the phase difference between the scattering surfaces oscillates increasingly faster as the eccentricity grows which is directly related to the oscillating nature of the phase factors $J_{n-m}(k_{c1}e)$, $J_{n-m}(k_{t1}e)$ and $J_{n-m}(k_{s1}e)$ present in the final equations (Hasheminejad and Badsar, 2004).

Fig.3 displays the variation of the backscattered far-field pressure amplitude with inclusion size for broadside/end-on incidence upon the compound cylinder at selected frequencies. Here, the eccentricity is kept fixed (e/a=0.5) while the radius of the inner cylinder is increased from b=0 to b=0.5a. The main observation is the relatively large (small) change in

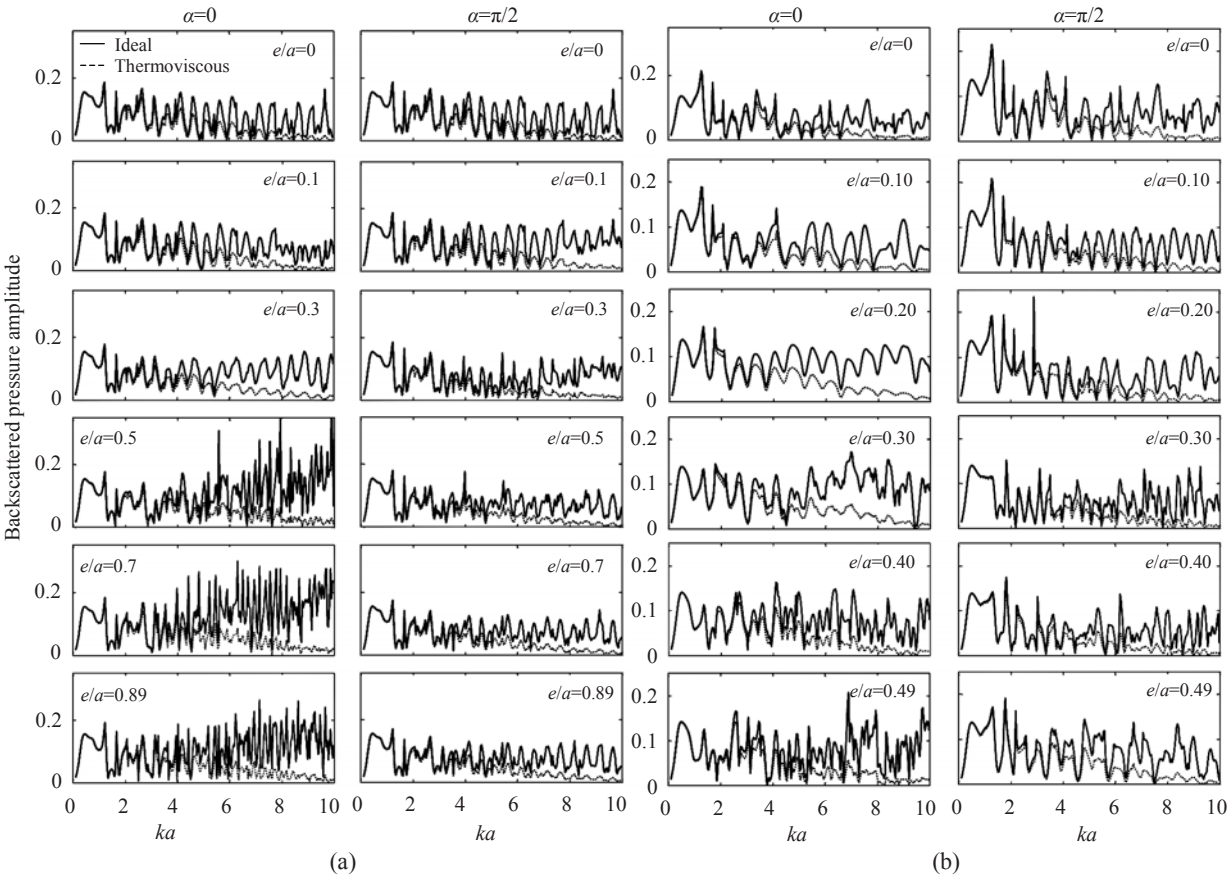

Fig.2 Variation of the normalized backscattered far-field acoustic pressure magnitude with dimensionless frequency for broadside/end-on incidence at selected eccentricities and inclusion size. (a) b=0.1a; (b) b=0.5a

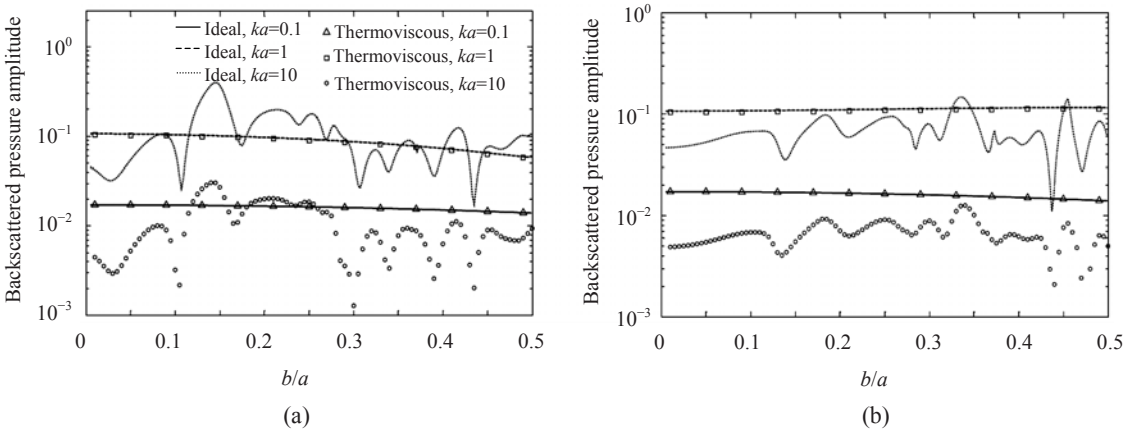

Fig.3 Variation of the backscattered far-field pressure amplitude with inclusion size for broadside/end-on incidence at selected frequencies and a fixed eccentricity (e/a=0.5). (a) α=0; (b) α=π/2

the backscattered pressure magnitude with inclusion size at high (low and intermediate) frequencies for both ideal and thermoviscous problems. The backscattered pressure curves associated with the end-on incidence (α=0) case at the highest frequency seem to be slightly more oscillatory (i.e., a higher variation in the backscattered pressure magnitude with inclusion size in the far-field point for end-on incidence is observed). The very inconsequential effect of thermoviscosity at low and intermediate frequencies is

once more noted, while there is roughly an order of magnitude downward shift in pressure amplitudes at the highest frequency for all inclusion sizes, regardless of angle of incidence. Also, numerical comparison of the ideal and thermoviscous pressure curves at the highest frequency reveals that thermoviscosity in general has a slightly higher effect on the overall backscattered pressure magnitudes for the cylinder containing a large inclusion in comparison with one with a small inclusion, especially in the broadside incidence ($\alpha=\pi/2$) case. This may be related to the high sound absorptive nature (i.e., very large thermoviscous parameters) of the core fluid (olive oil) in comparison with the coating fluid (FC-75).

To further investigate the effect of presence of core fluid in the compound thermoviscous cylinder, the angular distribution of the scattered far-field pressure amplitude at selected nondimensional frequencies (ka=0.1, 1, 10), inclusion sizes (b/a=0.1, 0.5), eccentricities and angles of incidence (α=0, π/2) are displayed in Figs.4a and 4b. It is interesting to study the change in directionality and amplitude of the scattered waves as the input parameters are varied. At the lowest frequency (ka=0.1), the scattered far-field pressure patterns are extremely uniform (nearly circular). At ka=1, the pressure patterns become more directional with still a very uniform forward scattering for both angles of incidence. At the highest frequency (ka=10), there is a significant decrease in the overall scattered pressure amplitudes (due to thermoviscous loss effects) while the patterns now exhibit a highly directional behaviour with a relatively sharp forward scattering in every case. The most important observation is perhaps the fact that while the eccentricity of a small inclusion (b/a=0.1) has almost no effect on the far-field scattered pressure directivities and amplitudes at low and intermediate frequencies, it has a perceptible effect at high frequencies, especially for the end-on incidence case. The situation is somewhat different for the large

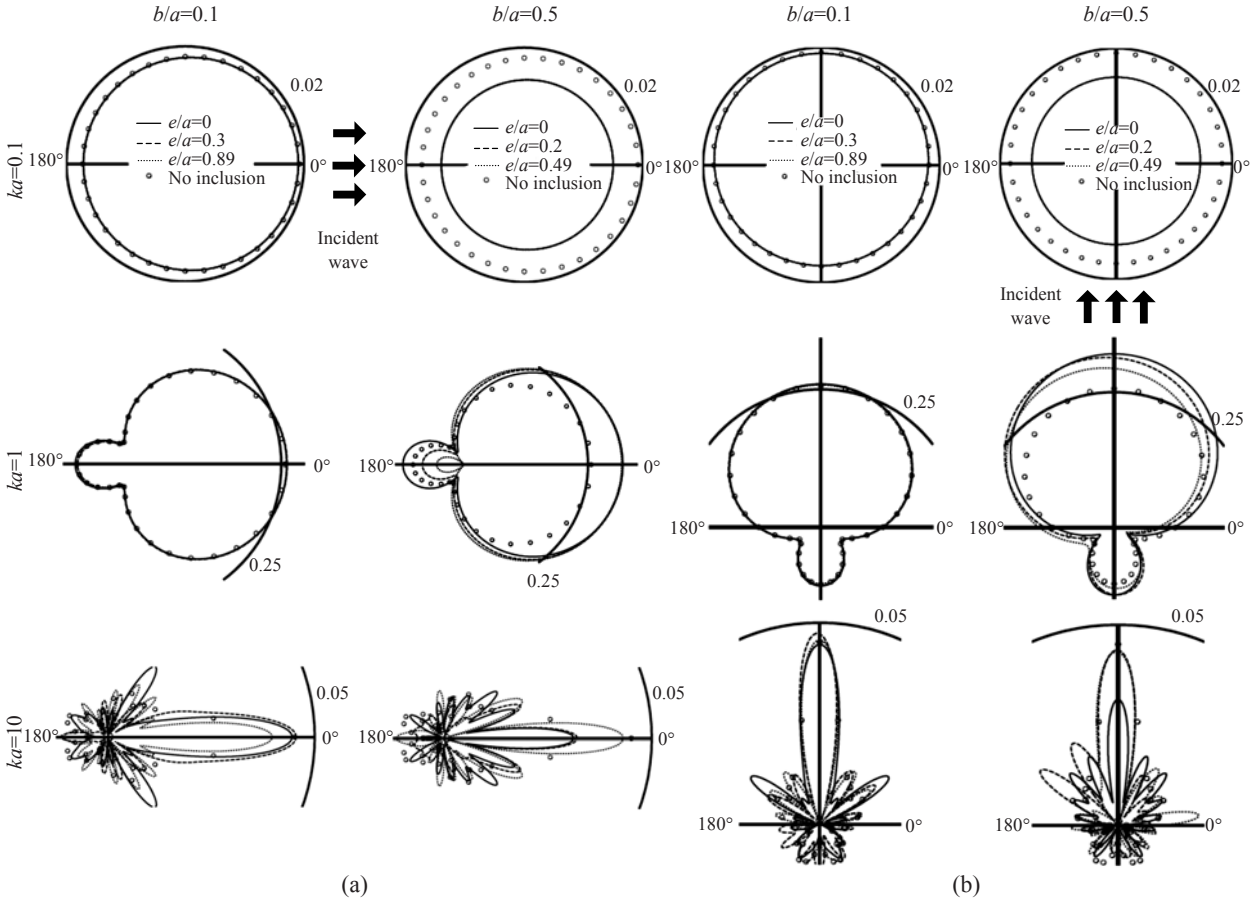

Fig.4 Angular distribution of the scattered far-field pressure amplitude at selected nondimensional frequencies, inclusion sizes and eccentricities for end-on incidence (α=0) (a) and for broadside incidence ($\alpha=\pi/2$) (b)

inclusion (b/a=0.5) on which the eccentricity has a small (considerable) effect at intermediate (high) frequencies. We lastly note that while the patterns are perfectly symmetric about the 180 degrees line in the end-on incidence case, they are slightly unsymmetric about the 90 degrees line in the broadside incidence situation (see Fig.1).

To assess the acoustic interaction effects in the near-field, the spatial distribution of the normalized total acoustic pressure magnitude, $|p(r_1,\theta_1,\omega)|/(\omega\rho_3\varphi_0)$, for end-on incidence ($\alpha$=0) at selected incident wave frequencies and eccentricities in the neighbourhood of the thermoviscous cylinder containing a large inclusion (b/a=0.5) is presented in Fig.5. The main observations are as follows. At the lowest frequency (ka=0.1), the pressure contours are highly non-directional and the highest pressure magnitude is observed in the forward direction. At this frequency the core eccentricity has nearly no effect on the total acoustic field. As the incident wave frequency is increased to ka=1 and 10, the directionality and overall magnitudes of the pressure field appreciably increase. At these frequencies, in contrast to the low frequency case, eccentricity of the core fluid has a noticeable effect on the pressure field. Another interesting aspect of the problem is the creation of shadow zones mainly in the forward direction behind the compound cylinder at intermediate and high frequencies. These regions are well-known to be of extra importance at high frequencies, as it is well known that waves whose wavelength is small in comparison to the obstacles suffer very large backscattering (create a strong shadow). At ka=1, core fluid eccentricity has a minor effect on the distinct U-shaped shadow region formed in the forward direction behind the compound cylinder. At the highest frequency (ka=10), effect of core eccentricity on the single (strip-shaped) shadow region formed behind the compound cylinder is extensive.

Finally, in order to check overall validity of the calculations, we computed the total scattering cross section [Eq.(34) in (Roumeliotis *et al*., 2001)] versus angle of plane wave incidence at selected radii ratios (b/a=0, 0.005, 0.01) and eccentricity (e/a=0.6) for a nearly inviscid and relatively large compound fluid cylinder immersed in an infinite ideal fluid medium by setting $\mu\to0$ in our main (thermoviscous) FORTRAN code. The numerical results, as shown in Fig.6, accurately reproduce the curves displayed in Fig.9b of (Roumeliotis and Kakogiannos, 1995). The

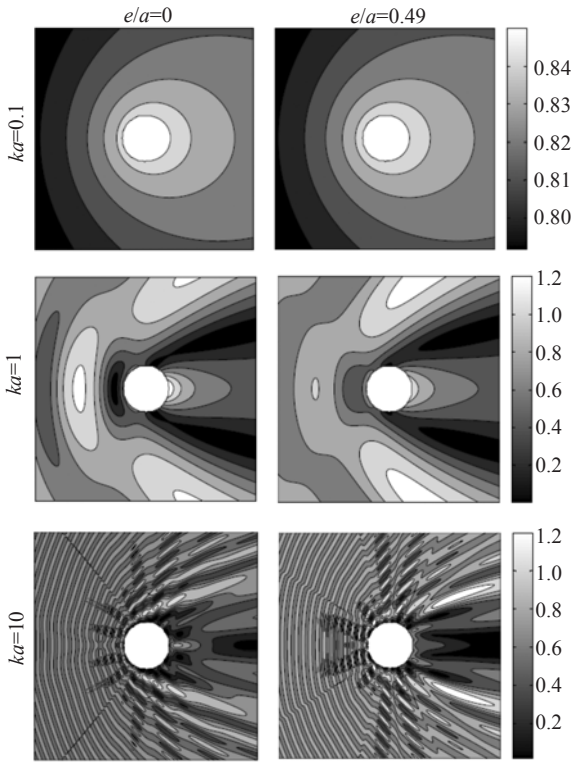

Fig.5 The spatial distribution of the normalized total acoustic pressure magnitude at selected incident wave frequencies and eccentricities for end-on incidence upon a compound thermoviscous cylinder containing a large inclusion (b/a=0.5)

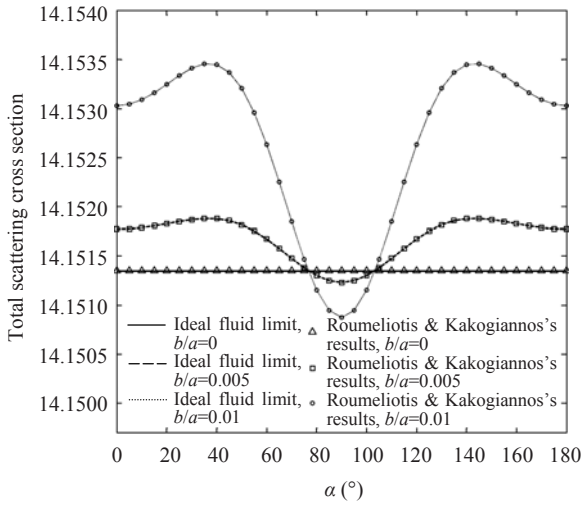

Fig.6 The total scattering cross section versus angle of incidence at selected radii ratios and eccentricity (e/a=0.6) for a nearly inviscid compound fluid cylinder immersed in an infinite fluid medium

remaining numerical results appearing in the latter reference were also readily reproduced (not shown for briefness) by using limiting input parameters values in our general thermoviscous code.

CONCLUSION

This study solves the most fundamental problem of acoustic scattering from eccentric fluid scatterers in 2D including dissipation effects. It treats the interaction of a plane compressional sound wave with a compound compressible fluid cylinder consisting of two parallel eccentric thermoviscous cylinders suspended in a boundless viscous thermally conducting fluid medium. The solution is based on the linearized coupled dynamic equations of thermoviscosity, the appropriate wave field expansions, the relevant boundary conditions and application of the translational addition theorem for cylindrical wave functions. The scattered far-field pressure amplitudes and the spatial distribution of total acoustic pressures are plotted for end-on/broadside incidence at selected incident wave frequencies, core sizes and eccentricities. The numerical results reveal the imperative influence of thermoviscosity in remarkable reduction of the backscattered pressure amplitudes at intermediate and high frequencies. These effects appear to generally enhance as the core fluid eccentricity is increased, especially for a large inclusion at end-on incidence. It has also been shown that the eccentricity of a small thermoviscous inclusion has a negligible (a perceptible) effect on the far-field scattered pressures at low and intermediate (high) frequencies. The situation is somewhat different for a large thermoviscous inclusion on which the eccentricity has a small (significant) effect at intermediate (high) frequencies. The numerical results are concluded with the field pressure contour plots illustrating emergence of considerable backscattering as well as the creation of distinct shadow zones behind the compound cylinder (in the forward direction) at intermediate and high frequencies. The presented work demonstrates the call for consideration of thermoviscous loss effects in combination with cross scattering interactions in problems involving eccentric absorptive fluid cylinders. It is of high practical interest in acoustic analysis and characterization of compound cylindrical emulsions, liquid composites, and passive acoustic stabilization of composite liquid bridges, small diffusion flames and hot cylindrical fluid objects under microgravity conditions.

ACKNOWLEDGMENT

The authors wish to greatly thank Professor David H. Bailey who assisted us with his powerful multi-precision FORTRAN software package for computing mathematical functions on floating point numbers of arbitrarily high precision.

References

Abramowitz, M., Stegun, I.A., 1965. Handbook of Mathematical Functions. National Bureau of Standards. Washington, DC.

Alemar, J.D., Delsanto, P.P., Rosario, E., Nagel, A., Uberal, H., 1986a. Spectral analysis of the scattering of acoustic waves from a fluid cylinder, I: Denser fluid loading. *Acustica*, **61**:1-6.

Alemar, J.D., Delsanto, P.P., Rosario, E., Nagel, A., Uberal, H., 1986b. Spectral analysis of the scattering of acoustic waves from a fluid cylinder, II: Denser fluid inside. *Acustica*, **61**:7-13.

Babick, F., Hinze, F., Ripperger, S., 2000. Dependence of ultrasonic attenuation on the material properties. *Colloids and Surfaces A: Physicochemical and Engineering Aspects*, **172**(1-3):33-46. [doi:10.1016/S0927-7757(00)00571-9]

Bailey, D.H., 1995. A FORTRAN-90 based multiprecision system. *ACM Trans. Math. Soft.*, **21**(4):379-387. [doi:10.1145/212066.212075]

Boag, A., Levitan, Y., Boag, A., 1988. Analysis of acoustic scattering from fluid cylinders using a multifilament source model. *J. Acoust. Soc. Am.*, **83**(1):1-8. [doi:10.1121/1.396422]

Cai, L.W., 2004. Multiple scattering in single scatterers. *J. Acoust. Soc. Am.*, **115**(3):986-995. [doi:10.1121/1.1643362]

Chandra, K., Thompson, C., 1992. Improved perturbation method for scattering from a fluid cylinder. *J. Acoust. Soc. Am.*, **92**(2):1047-1055. [doi:10.1121/1.404034]

Chung, S.K., Trinh, E.H., 1998. Containerless protein crystal growth in rotating levitated drops. *J. Cryst. Growth*, **194**(3-4):384-397. [doi:10.1016/S0022-0248(98)00542-9]

Danila, E.B., Conoir, J.M., Izbicki, J.L., 1995. Generalized Debye series expansion: Treatment of the concentric and nonconcentric cylindrical fluid-fluid interfaces. *J. Acoust. Soc. Am.*, **98**(6):3326-3342. [doi:10.1121/1.413820]

Danila, E.B., Conoir, J.M., Izbicki, J.L., 1998. Generalized Debye series expansion. Part II, Treatment of eccentric fluid-solid cylindrical interfaces. *Acta Acustica*, **84**:38-44.

Doi, T., Koster, J.N., 1993. Thermocapillary convection in two immiscible liquid layers with free surface. *Phys. Fluids A*, **5**(8):1914-1927.

Dongarra, J., Bunch, J., Moler, C., Stewart, G.W., 1979. LINPACK User's Guide. SIAM.

Eyer, A., Leiste, H., 1985. Striation-free silicon crystal by float-zoning with surface coated melt. *J. Cryst. Growth*, **71**(1):249-252. [doi:10.1016/0022-0248(85)90073-9]

Faran, J.J., 1951. Sound scattering by solid cylinders and spheres. *J. Acoust. Soc. Am.*, **23**(4):405-418. [doi:10.1121/1.1906780]

Gao, J.R., Wei, B.B., 1999. Containerless solidification of undercooled NdFeZrB alloy droplets in a drop tube. *J. Alloys Compd.*, **285**(1-2):229-232. [doi:10.1016/S0925-8388(98)00870-6]

Hasegawa, T., Yasutaka, H., Akio, H.A., Hideki, N., Massahiko, K., 1993. Acoustic radiation pressure acting on spherical and cylindrical shells. *J. Acoust. Soc. Am.*, **93**(1):154-160. [doi:10.1121/1.405653]

Hasheminejad, M., Geers, T.L., 1993. Modal impedance for two spheres in a thermoviscous fluid. *J. Acoust. Soc. Am.*, **94**(4):2205-2214. [doi:10.1121/1.407491]

Hasheminejad, M., Azarpeyvand, M., 2003. Energy distribution and radiation loading of a cylindrical source suspended within a nonconcentric fluid cylinder. *Acta Mechanica*, **164**(1-2):15-30. [doi:10.1007/s00707-003-0014-9]

Hasheminejad, M., Badsar, A., 2004. Acoustic scattering by a pair of poroelastic spheres. *Quart. J. Mech. Appl. Math.*, **57**(1):95-113. [doi:10.1093/qjmam/57.1.95]

Janele, P.J., Mioduchowski, A., Haddow, J.B., 1991. A note on finite dynamic deformation of concentric cylinders. *Int. J. Eng. Sci.*, **29**(12):1585-1592. [doi:10.1016/0020-7225(91)90128-P]

Johnson, D.T., 2002. Viscous effects in liquid encapsulated liquid bridges. *Int. J. Heat Fluid Flow*, **23**(6):844-854. [doi:10.1016/S0142-727X(02)00186-8]

Kanevskii, I.N., Surikov, B.S., 1976. Two-layer acoustic lenses. *Acoustics*, **22**:292-294.

Lamb, H., 1945. Hydrodynamics. Dover.

Lane, M., Forest, K.T., Lyons, E.A., Bavister, B.D., 1999. Live births following vitrification of hamster embryos using a novel containerless technique. *Theriogenology*, **51**(1):167. [doi:10.1016/S0093-691X(99)91726-0]

Li, M.W., Zeng, D.L., Zhu, T.X., 2002. Instability of the Marangoni convection in a liquid bridge with liquid encapsulation under microgravity condition. *Int. J. Heat Mass Transfer*, **45**(1):157-164. [doi:10.1016/S0017-9310(01)00125-9]

Li, Y.R., Liu, Y.J., Peng, L., Wang, Y., 2006. Three-dimensional oscillatory thermocapillary flow in encapsulated liquid bridge. *Phys. Fluids*, **18**(7):074108-1-074108-6. [doi:10.1063/1.2227051]

Lin, W.H., Raptis, A.C., 1983. Acoustic scattering by elastic solid cylinders and spheres in viscous fluids. *J. Acoust. Soc. Am.*, **73**(3):736-748. [doi:10.1121/1.389039]

Lorber, B., Giege, R., 1996. Containerless protein crystallization in floating drops—Application to crystal-growth monitoring under reduced nucleation conditions. *J. Cryst. Growth*, **168**(1-4):204-215. [doi:10.1016/0022-0248(96)00356-9]

Mai, J., Yamane, R., Früh, W.G., Oshima, S., Ando, A., 2002. Unstable waves at the interface of a diamagnetic liquid column contained in a magnetic fluid. *European Journal of Mechanics-B/Fluids*, **21**(2):237-246. [doi:10.1016/S0997-7546(01)01168-2]

Marr-Lyon, M.J., Thiessen, D.B., Marston, P.L., 1997. Stabilization of a cylindrical capillary bridge far beyond the Rayleigh-Plateau limit using acoustic radiation pressure and active feedback. *J. Fluid Mech.*, **351**:345-357. [doi:10.1017/S002211209700726X]

Marr-Lyon, M.J., Thiessen, D.B., Blonigen, F.J., Marston, P.L., 2000. Stabilization of electrically conducting capillary bridges using feedback control of radial electrostatic stresses and the shapes of extended bridges. *Phys. Fluids*, **12**(5):986-995. [doi:10.1063/1.870354]

Marr-Lyon, M.J., Thiessen, D.B., Marston, P.L., 2001. Passive stabilization of capillary bridges in air with acoustic radiation pressure. *Phys. Rev. Lett.*, **86**(11):2293-2296. [doi:10.1103/PhysRevLett.86.2293]

Montanero, J.M., 2003. Theoretical analysis of the vibration of axisymmetric liquid bridges of arbitrary shape. *Theoret. Comput. Fluid Dynamics*, **16**(3):171-186. [doi:10.1007/s00162-002-0077-6]

Montanero, J.M., Cabezas, G., Acero, J., Perales, J.M., 2002. Theoretical and experimental analysis of the equilibrium contours of liquid bridges of arbitrary shape. *Phys. Fluids*, **14**(2):682-693. [doi:10.1063/1.1427922]

Morse, P., Ingard, K., 1968. Theoretical Acoustics. McGraw-Hill.

Morse, S.F., Feng, Z.W., Marston, P.L., 1995. High-frequency threshold processes for leaky waves on cylinders of variable thickness: Fluid shell case. *J. Acoust. Soc. Am.*, **98**(5):2928. [doi:10.1121/1.414135]

Moseler, M., Landman, U., 2000. Formation, stability, and breakup of nanojets. *Science*, **289**(5482):1165-1169. [doi:10.1126/science.289.5482.1165]

Nagashio, K., Takamura, Y., Kuribayashi, K., Shiohara, Y., 1999. Microstructural control of $NdBa_3Cu_3O_7$-delta superconducting oxide from highly undercooled melt by containerless processing. *J. Cryst. Growth*, **200**(1-2):118-125. [doi:10.1016/S0022-0248(98)01258-5]

Perales, J.M., Meseguer, J., 1992. Theoretical and experimental study of the vibration of axisymmetric viscous liquid bridges. *Phys. Fluids A*, **4**(6):1110-1130.

Rayleigh, L., 1945. Theory of Sound. Dover.

Reese, J.M., Thompson, W., 1986. Acoustic diffraction by a variable thickness fluid layer. *J. Acoust. Soc. Am.*, **80**(6):1810-1815. [doi:10.1121/1.394295]

Rhim, W.K., Ohsaka, K., Paradis, P.F., Spjut, R.E., 1999. Noncontact technique for measuring surface-tension and viscosity of molten materials using high-temperature electrostatic levitation. *Rev. Sci. Instrum.*, **70**(6):2796-2801. [doi:10.1063/1.1149797]

Roumeliotis, J.A., Kakogiannos, B., 1995. Acoustic scattering from an infinite cylinder of small radius coated by a penetrable one. *J. Acoust. Soc. Am.*, **97**(4):2074-2081. [doi:10.1121/1.412000]

Roumeliotis, J.A., Ziotopoulos, A.P., Kokkorakis, G.C., 2001. Acoustic scattering by a circular cylinder parallel with another of small radius. *J. Acoust. Soc. Am.*, **109**(3):870-877. [doi:10.1121/1.1348296]

Rousselot, J.L., 1994. Field diffracted by a fluid cylinder: Comparison between the geometrical theory of diffraction and a model solution. *Acustica*, **80**:14-20.

Sanz, A., 1985. The influence of the outer bath in the dynamics of axisymmetric liquid bridges. *J. Fluid. Mech.*, **156**:101-140. [doi:10.1017/S0022112085002014]

Schuster, G.T., 1990. A fast exact numerical solution for the acoustic response of concentric cylinders with penetrable interfaces. *J. Acoust. Soc. Am.*, **87**(2):495-502. [doi:10.1121/1.398919]

Scotti, T., Wirgin, A., 2004. Reconstruction of the three mechanical material constants of a lossy fluid-like cylinder from low-frequency scattered acoustic fields. *Comptes Rendus Mécanique*, **332**(9):717-724. [doi:10.1016/j.crme.2004.03.018]

Shaw, R.P., Tai, G., 1974. Time harmonic acoustic radiation from nonconcentric circular cylinder. *J. Acoust. Soc. Am.*, **56**(5):1437-1443. [doi:10.1121/1.1903462]

Sinai, J., Waag, R.C., 1988. Ultrasonic scattering by two concentric cylinders. *J. Acoust. Soc. Am.*, **83**(5):1728-1735. [doi:10.1121/1.396505]

Stratton, J.A., 1941. Electromagnetic Theory. McGraw-Hill.

Temkin, S., 1981. Elements of Acoustics. Wiley, New York.

Thiessen, D.B., Marr-Lyon, M.J., Marston, P.L., 2002. Active electrostatic stabilization of liquid bridges in low gravity. *J. Fluid Mech.*, **457**:285-294. [doi:10.1017/S0022112002007760]

Varadan, V.V., Ma, Y., Varadan, V.K., Lakhtakia, A., 1991. Scattering of Waves by Spheres and Cylinders. *In*: Varadan, V.V., Lakhtakia, A., Varadan, V.K. (Eds.), Field Representation and Introduction to Scattering. Elsevier, Amsterdam, p.211-324.

Viviani, A., Golia, C., 2003. Thermocapillary flows in two-fluids liquid bridges. *Acta Astronautica*, **53**(11):879-897. [doi:10.1016/S0094-5765(02)00240-0]

Walker, J.S., Henry, D., BenHadid, H., 2002. Magnetic stabilization of the buoyant convection in the liquid-encapsulated Czochralski process. *J. Cryst. Growth*, **243**(1):108-116. [doi:10.1016/S0022-0248(02)01487-2]

Wei, W., Thiessen, D.B., Marston, P.L., 2004. Acoustic radiation force on a compressible cylinder in a standing wave. *J. Acoust. Soc. Am.*, **116**(1):201-208. [doi:10.1121/1.1753291]

Zayas, F., Alexander, J.I.D., Meseguer, J., Ramus, J.F., 2000. On the stability limits of long nonaxisymmetric cylindrical liquid bridges. *Phys. Fluids*, **12**(5):979-985. [doi:10.1063/1.870353]

Zhang, S., Jin, J., 1996. Computation of Special Functions. John Wiley & Sons.